

1 **Simulation of spatial and temporal trends in nitrate concentrations at the regional**
2 **scale in the Upper Dyle Basin, Belgium'**

3

4 César E.^{1,*}, Wildemeersch S.¹, Orban Ph.¹, Carrière S.², Brouyère S.¹, Dassargues A.¹

5 ¹University of Liege, ArGEnCo, GEO³; Hydrogeology and Environmental Geology, Aquapôle, B52/3
6 Sart-Tilman, 4000 Liege, Belgium

7 ²UMR 1114 EMMAH (UAPV-INRA), Université d'Avignon et des Pays de Vaucluse, 33 rue Pasteur,
8 84 000 Avignon, France

9 *corresponding author

10 Address: University of Liege, ArGEnCo, GEO³; Hydrogeology and Environmental Geology, Aquapôle,
11 B52/3 Sart-Tilman, 4000 Liege, Belgium

12 E-mail (work): cesar.emilie@gmail.com

13 Phone number (work): +32(0)43662308

14 Fax number (work): +32(0)43669520

15 **Abstract**

16 Models are the only tools capable of predicting the evolution of groundwater systems at a regional
17 scale in taking into account a large amount of information. This study presents the association of a
18 water balance model (WetSpass) with a groundwater flow and solute transport model (SUFT3D,
19 « *Saturated and Unsaturated Flow and Transport in 3D* ») in order to simulate the present and future
20 groundwater quality in terms of nitrate in the Upper Dyle basin (439 km², Belgium). The HFEMC
21 (« *Hybrid Finite Element Mixing Cell* ») method implemented in the SUFT3D code is used to model
22 groundwater flow and nitrate transport. A spatially-distributed recharge modelled with WetSpass is
23 considered for prescribing the recharge to the groundwater flow model. The feasibility of linking
24 WetSpass model with the finite-elements SUFT3D code is demonstrated. Time evolution and
25 distribution of nitrate concentration are then simulated using the calibrated model. Nitrate inputs are
26 spatially-distributed according to land use. The spatial simulations and temporal trends are compared
27 with previously published data on this aquifer and show good results.

28 **Key words:** groundwater modelling, nitrate, WetSpass, spatially-distributed recharge, Belgium.

29

30 **1. Introduction**

31 When a contaminant enters a groundwater system, its residence time varies enormously. Water may
32 spend as little as days or weeks underground or the residence time can be of the order of a few
33 decades (Peeters, 2010) or longer. Consequently, efforts are needed to reliably assess the impact of
34 groundwater contamination, especially by nitrates which have been identified as one of the most
35 problematic and widespread diffuse pollutants of groundwater (e.g. Mitchell et al. 2003; Mohamed et
36 al. 2003; Thorburn et al. 2003; Oren et al. 2004; Jackson et al. 2008; Visser et al. 2009; Sutton et al.
37 2011). Groundwater contamination by nitrates is primarily linked to anthropogenic activities such as
38 disposal of organic wastes, and mainly the use of fertilizers for agriculture (Hallberg and Keeney 1993;
39 Hudak 2000; Harter et al. 2002; Johnsson et al. 2002; Collins and McGonigle 2008, Wick et al. 2012).
40 This nitrate contamination of groundwater can lead to health problems when drinking water is
41 considered. Additionally, nitrate contamination of groundwater can also lead to huge ecological
42 problems, such as eutrophication. Due to this problematic, it is essential to develop integrated
43 management tools capable of identifying the fate of nitrate in groundwater and the link between the
44 use of nitrogen fertilizers and the resulting evolution of nitrate concentration in groundwater. The only

45 tools capable of achieving such objectives by taking into account many piece of information gathered
46 on a groundwater system for predicting its future evolution are numerical models.

47

48 This paper presents a modelling approach for predicting the evolution of groundwater quality trend at
49 the regional scale by linking a soil water balance model and a groundwater flow and transport model.
50 Obtained results are presented for the Upper Dyle basin (439 km², Belgium). The specific objectives of
51 this paper consist in (i) demonstrating the feasibility of associating a soil water balance model
52 (WetSpass, « *Water and Energy Transfer between Soil, Plants and Atmosphere under quasi-Steady-*
53 *State* ») with a groundwater flow finite-elements model (SUFT3D, « *Saturated and Unsaturated Flow*
54 *and Transport in 3D* »), (ii) from this association, modelling the groundwater flow using a spatial
55 distribution of recharge calculated from the soil water balance WetSpass model, in one hand, and
56 simulating the transport of nitrate in the basin using a spatial distribution of the nitrate loads according
57 to land use, in the other hand, and, (iii) comparing the simulated spatial and temporal trends with
58 previously published data on this aquifer. Therefore, the main objective of this paper is to show the
59 actual feasibility of the considered methodology for the simulation of nitrate trend at the regional scale
60 and to illustrate it on a representative basin. Limitations of this methodology will be developed in the
61 discussion section.

62

63 Approaches commonly used to model groundwater flow and transport at regional scale can be
64 classified into three categories: black-box models, sometimes called lumped-parameter models or
65 transfer functions (e.g. Jury 1982; Maloszewski and Zuber 1982; Amin and Campana 1996; Skaggs *et*
66 *al.* 1998; Stewart and Loague 1999; Yi and Lee 2004), compartment models (e.g. Barrett and
67 Charbeneau 1996; Campana *et al.* 1997; Harrington *et al.* 1999; Rozos and Koutsoyiannis 2006), and
68 physically-based and spatially-distributed models (e.g. Dassargues *et al.* 1988; Therrien and Sudicky
69 1996; Sophocleous *et al.* 1999; Henriksen *et al.* 2003). With black-box models, systems are
70 considered as a whole, and inputs and outputs are linked with transfer functions (Ledoux 2003). As no
71 information is derived from the spatial distribution and time evolution of the parameters, predictive
72 capability of such model are relatively limited (Orban *et al.* 2008). Consequently, they are generally not
73 used in hydrogeology, apart for karstic systems, for which the mechanisms are so complex that
74 parameterisation becomes difficult. Compartment models are usually made of “black-box” models

75 connected in series or spatially-distributed. However, flow and transport processes are still
76 represented by semi-empirical transfer functions. Physically-based and spatially-distributed models
77 are based on the resolution of spatially-distributed 2D or 3D equations of groundwater flow and solute
78 transport. Such models usually offer a high flexibility in terms of processes, boundary conditions, and
79 stress factors. They have good predictive capabilities and their results are spatially-distributed.
80 However, they require large data sets and detailed information on the system such as geological
81 maps, hydraulic head, flow rate data, hydrogeological parameter values and their spatial distribution
82 (hydraulic conductivity, storage coefficient, effective porosity, dispersivity coefficients) (Barthel *et al.*
83 2008). In principle, all these parameters can be measured but in practice, large scale field
84 investigations are not easily feasible. Physically-based and spatially-distributed models are also very
85 time-consuming due to the complicated parameterisation and prone to numerical problems such as
86 instability and numerical dispersion. The innovative HFEMC (« **Hybrid Finite Element Mixing Cell** »)
87 method (Brouyère *et al.* 2009; Wildemeersch *et al.* 2010; Orban *et al.* 2010), implemented in SUFT3D
88 code (Carabin and Dassargues 1999; Brouyère 2001; Brouyère *et al.* 2004), is a compromise between
89 black-box models and physically-based and spatially-distributed models that offers a pragmatic
90 solution to the issues encountered in groundwater flow and transport modelling at regional scale.

91
92 The deterministic approach developed here allows estimating the space-time fate of nitrate in
93 groundwater quite rapidly. A wide range of nutrient balance models based on deterministic process
94 have also been developed (Diekkrüger *et al.* 1995). More specifically, a significant body of research
95 has been done on nitrate transport within the Dyle catchment. Navarre *et al.* (1976) published the
96 results of an important sampling campaign in the Dyle watershed. Pineros-Garcet *et al.* (2006)
97 developed a mathematical definition for metamodels of nitrogen leaching from soils and crop rotations
98 in the area of the Brusselian aquifer in Belgium. Similarly, Mattern (2009) worked on the Brusselian
99 sand groundwater body in order to map the nitrate concentrations in the aquifer as well as identify
100 sources of groundwater nitrate pollution. More recently, Peeters (2010) developed a methodology to
101 identify and quantify natural and anthropogenic contributions to the groundwater chemical composition
102 of the Brussel sands aquifer. A number of conceptual geochemical models were implemented
103 numerically and the uncertainty was incorporated explicitly in the prediction.

104

105 The recharge constitutes an indispensable input for the implementation of a groundwater flow or
106 transport model. The recharge is the downward flow of water reaching the groundwater level and
107 forming an addition to the groundwater reservoir. At the regional scale, parameters governing the
108 recharge are space dependent and taking into account its spatial variability is essential for both
109 groundwater flow and solute transport regional modelling (Batelaan and De Smedt 2007). Methods for
110 estimating recharge have been discussed in several papers (e.g. Scanlon *et al.* 2002; Batelaan and
111 De Smedt 2007; USGS 2009; Healy 2010). These approaches can be grouped into five classes: (1)
112 water balance techniques, (2) determination from surface water data, (3) techniques based on the
113 study of the saturated zone (Darcy law or observations of piezometric fluctuations), (4) determination
114 from environmental tracers, and (5) inverse modelling. The selection of one method is largely driven
115 by the goals of the study (mainly the time and space scale) and the validity of the technique (Healy
116 2010). Recharge can also be determined indirectly with fully integrated physically-based models.
117 These ones attempt to account for all interactions between surface and subsurface flow regimes.
118 HydroGeoSphere, for example, is a model which is able to simulate water flow in a fully integrated
119 mode, thus allowing precipitation to partition into all key components of the hydrologic cycle, including
120 recharge (Brunner and Simmons 2012; Therrien *et al.* 2005). According to Batelaan and De Smedt
121 (2007), spatially-distributed water balance models are the most appropriate to estimate recharge at
122 regional scale. Moreover, it is a common and flexible approach giving good results provided that the
123 components of the water balance are accurate. In this context, the WetSpass model (Batelaan and De
124 Smedt 2001; Batelaan and De Smedt 2003; Batelaan and De Smedt 2004; Batelaan and De Smedt
125 2007; Dams *et al.* 2007; Jenifa Latha *et al.* 2010 ; Wang *et al.* 2010) constitutes an interesting
126 approach that will be used to reach the objectives of this work.

127

128 **2. Methodology**

129 **2.1. The HFEMC method**

130 The HFEMC method is based on the finite element formalism and is implemented in the SUFT3D code
131 developed by the group of Hydrogeology and Environmental Geology at the University of Liège
132 (Carabin and Dassargues 1999; Brouyère 2001; Brouyère *et al.* 2004). The SUFT3D fully treats 3D
133 problems under steady-state or transient conditions. The code uses the Control Volume Finite Element
134 method (CVFE) to solve the groundwater flow equation based on the mixed formulation of Richard's

135 equation proposed by Celia *et al.* (1990). The flow in the unsaturated media is therefore also
136 considered in the groundwater model. Transport processes considered in the code include advection,
137 hydrodynamic dispersion, first order degradation, equilibrium sorption (linear, Freundlich or Langmuir
138 isotherms) and a physical non-equilibrium first-order dual-porosity model (Brouyère 2001).

139

140 The HFEMC method is a flexible technique combining the advantages of both black-box models and
141 physically-based and spatially-distributed models (Brouyère *et al.* 2009). This method allows defining a
142 conceptual, mathematical and numerical approach for each type of contexts of the studied region
143 (Orban *et al.* 2010). The principle is to subdivide the modelled zone into several subdomains and then
144 to select specific groundwater flow and transport equations for each subdomain, depending on the
145 available data and on the relative hydrogeological complexity. The available numerical formulations for
146 solving the groundwater flow problem are a linear reservoir, spatially-distributed reservoirs, and the
147 groundwater flow equation in porous media. Similarly, three formulations are implemented to solve the
148 solute transport problem, a linear reservoir, spatially-distributed mixing cells or the advection-
149 dispersion equation. A series of internal boundary conditions can be defined at the interfaces between
150 subdomains as well as between groundwater and surface for modelling exchange of water and solute.
151 First type dynamic boundary conditions (Dirichlet) are defined where continuity in hydraulic heads is
152 assumed across the interface boundary. The term dynamic is used to highlight that the hydraulic head
153 remains a time-varying unknown of the problem. Second type boundary conditions (Neumann) are
154 defined along interface boundaries where there is no groundwater and no solute exchange between
155 the subdomains (first derivative of hydraulic head set equal to 0). Third type dynamic boundary
156 conditions (Cauchy) are prescribed at interface boundaries where the exchanged groundwater flux is
157 calculated based on the difference in hydraulic heads across the boundary and a first-order transfer
158 coefficient. Associated nitrate mass fluxes are also computed. A full description of the HFEMC method
159 including the full set of used equations is provided in Brouyère *et al.* (2009) and Orban (2008).

160

161 **2.2. The WetSpass model**

162 The WetSpass model is a physically-based water balance model developed by Batelaan and De
163 Smedt (2001). This is a tool to estimate the temporal average and spatial distribution of surface runoff,
164 actual evapotranspiration, and groundwater recharge in steady-state conditions (annual or biannual

165 scale), using average climate, topographic, piezometric, land use and soil data. This approach is
166 flexible and takes into account the spatial variation of the processes related to the recharge (Batelaan
167 and Woldeamlak 2007). The simulated recharge can be used as an input for a groundwater model
168 (Batelaan and De Smedt 2007; Dams *et al.* 2007; Jenifa Latha *et al.* 2010 ; Wang *et al.* 2010). The
169 basin or region is considered as a regular pattern of raster cells, further subdivided in a vegetated,
170 bare soil, open water and impervious surface fractions for which independent water balances are
171 calculated (Batelaan and De Smedt 2007). The water balance of a cell is simply the sum of the water
172 balances of each fractions of the cell. For more details about the methodology, see Batelaan and De
173 Smedt (2001), Batelaan and De Smedt (2007), and Batelaan and Woldeamlak (2007).

174

175 **3. Application on the upper Dyle basin**

176 **3.1. Geographical, geological, and hydrogeological context**

177 The Dyle basin is located in the central zone of Belgium (Figure 1). For this study, only the upper basin
178 is considered, in which the Dyle stream has a length of 35 km. The upper basin is about 439 km². The
179 elevation ranges from 35 to 175 m with an average of 122 m. Given the latitude and the proximity to
180 the sea, the climate is maritime humid temperate characterised by average annual temperature of
181 10°C (Walloon Region 2005). Average rainfall corresponds to 830 mm/year and actual
182 evapotranspiration is estimated to 550 mm/year (*ibid.*). More than half of the surface of the Dyle basin
183 is covered by agriculture (57 % in 2008, Figure 1). Since agriculture constitutes one of the main source
184 of groundwater nitrate contamination (DGARNE 2010), the Dyle basin is an interesting region for such
185 a study. Several studies showed that concentrations of more than the norm of 50 mg/L have been
186 observed in groundwater (Sohier *et al.* 2009 ; Mattern *et al.* 2009)

187 **Figure 1. Landuse and location of the upper Dyle basin in Belgium**

188

189 Geologically, nearly horizontal layers of the Cenozoic and Mesozoic eras overlie the highly fractured
190 Paleozoic bedrock (Houthuys *et al.* 2011). Cenozoic formations are Paleogene clays and sands
191 (Brussels sands), extended homogeneously. Mesozoic era is represented by Cretaceous chinks,
192 located in the north part of the basin. Typical cross-sections show that the rivers are draining
193 Paleogene sands, Cretaceous chinks and the Paleozoic bedrock (Figure 2). The fractured Paleozoic
194 bedrock constitutes a low permeability basement, depending on the fracturation and nature of the

195 rocks. Two main aquifers can be highlighted, the first one in the Cretaceous chalk, the second one in
196 the Brussels sands. These two aquifers are locally separated by a thin clay layer of low permeability
197 as described in Dassargues and Ruthy (2001 and 2002). The hydraulic gradient of groundwater flow is
198 very low on the interfluvies and very steep close to rivers and discharge zones (Peeters 2010, Peeters
199 *et al.* 2010).

200 **Figure 2. Typical geological profiles in the upper Dyle basin and piezometric map (average mid-**
201 **seventies to 2007), according to Peeters (2010)**

202

203 **3.2. Spatially-distributed recharge determination**

204 The recharge was calculated using the WetSpass model. This study considered two hydrological
205 seasons, with summer ranging from April to September and winter from October to March, similarly to
206 the study of Batelaan and De Smedt (2007). A large set of data is required to run WetSpass. The pre-
207 processing used to create the inputs as well as the data needed are listed in Table 1. As shown in
208 Table 1, different interpolations methods were undertaken. Consequently, ten WetSpass models
209 resulting from the ten combinations of the meteorological data interpolations were tested. Figure 3
210 gives an example of all raster data needed for modelling the recharge, in addition to land use data,
211 piezometry (already shown in Figures 1 and 2) and wind speed. In Figure 3, temperature, precipitation
212 and evapotranspiration are interpolated by the inverse distance weighted method.

213 **Table 1. Data needed and methods used to estimate WetSpass inputs**

214

215 **Figure 3. Example of input raster data used for the implementation of the WetSpass model**
216 **(piezometry, land use and wind excepted)**

217

218 The application of the WetSpass model with the different combinations of inputs has a similar mean
219 global annual recharge. It was found that maize and tuberous areas are the first contributors to
220 groundwater recharge, with a mean of 363 mm/year against 270 mm/year for other diverse crops. It is
221 interesting to note that maize and tuberous are associated with a higher charge in nutritive elements
222 and so, a higher risk for groundwater (Batelaan and De Smedt 2007). On the contrary, urban areas
223 correspond to low recharge zones, with a mean of 160 mm/year. The comparison of the recharge
224 results presented in Figure 4 with literature (Meyus *et al.* 2004; Batelaan and De Smedt 2007; Peeters

225 2010) showed that the WetSpass model was applied correctly and that the spatially-distributed
226 recharge could be used as an input for the hydrogeological model.

227 **Figure 4. Annual recharge calculated by the WetSpass model**

228

229 **3.3. Numerical model**

230 The Upper Dyle basin model consists in a 3D regional model containing two layers. The model limits
231 are the catchment boundaries. A zero flow second type boundary condition was thus prescribed,
232 considering that there is no groundwater and not solute exchange with the neighbouring watersheds,
233 except for a 8 km long portion where the Dyle basin gains a flux of 0.33 m³/s from the neighbouring
234 Gette watershed (Dassargues *et al.* 2001). In this portion, the surface water divide does not coincide
235 with the groundwater divide, as shown by Peeters (2010). For this portion, a third type boundary
236 condition was prescribed, the exchanged groundwater flux being calculated based on the difference in
237 hydraulic heads across the boundary and a first-order transfer coefficient (Figure 5). The bottom layer
238 contains three facies: the Paleozoic basement, the Cretaceous chinks in the North and the
239 Carboniferous limestones in the South. The upper layer is composed by the Brussels sands and the
240 alluvial formations and is divided into seven different materials (Figure 6). A total of 11 subdomains are
241 considered; the area being first divided into three sub-basins where baseflow rates measurements are
242 available for calibration and then further subdivided to take into account the presence or absence of
243 clay. Internal first type *dynamic* boundary conditions are prescribed between these subdomains to
244 assume the continuity in hydraulic heads across the interface boundary. The thin clay layer locally
245 separating the upper aquifer (Brussels sands) from the lower aquifer (Cretaceous chinks) is
246 represented using a conductance coefficient that depends on the local thickness and hydraulic
247 conductivity of the clay layer. Volumes extracted in pumping wells were calculated on the basis of a
248 database. The 3D mesh is composed of 12,750 elements and 9,933 nodes.

249 **Figure 5. Internal and external boundary conditions used for the groundwater flow modelling of**
250 **the upper Dyle basin**

251 **Figure 6. 3D finite element mesh and zonation used for the groundwater flow modelling of the**
252 **upper Dyle basin**

253

254 A solute transport model is used for simulating the spatial and temporal long term evolution of nitrates
255 at regional scale. Therefore, short term concentration variations associated to piezometric variations
256 are not considered to be reproduced. Consequently, a steady-state simulation can be supposed
257 acceptable to represent average conditions for the considered period. Transient conditions are used to
258 model nitrate transport in order to reproduce the general nitrate concentration evolution over time
259 (Orban *et al.* 2010).

260

261 The HFEMC technique has been applied in the present study for its ability to combine a classical
262 approach, based on the calculation of the Richard's equation, for modelling the groundwater flow, and
263 a simplified approach, based on the mixing cell technique, to model solute transport. The relatively
264 high level of knowledge about hydrogeological conditions in the Dyle basin allows solving the
265 groundwater flow problem using the classical spatially-distributed groundwater flow. For the solute
266 transport problem, solving the advection-dispersion equation at regional scale remains a huge
267 challenge from a numerical point of view. However, considering that the main source of nitrate in the
268 Dyle basin comes from agriculture, the nitrate pollution can be considered as diffuse and, in this
269 particular case, the hydrodynamic dispersion in groundwater will be negligible with regards to the
270 dispersion of the source (Duffy and Lee 1992; Orban *et al.* 2010). Consequently, the spatially-
271 distributed mixing cell equation is selected as a good compromise between accuracy, robustness, and
272 physical soundness to model nitrate transport at the regional scale (Orban *et al.* 2010). Without any
273 denitrification evidences (oxic conditions clearly prevail throughout the aquifer), nitrate is assumed to
274 be conservative in the aquifers of the Dyle basin (no degradation) (Christakos and Bogaert 1996;
275 Mattern *et al.* 2009).

276

277 Data used to implement the hydrogeological model concern primarily the geometry and the geology,
278 the flow parameter values (hydraulic conductivity and effective porosity), the stress factors (recharge
279 resulting from the application of the WetSpas model and pumping flow rates) and historical data
280 concerning measured hydraulic heads, stream flow rates, and solute concentrations (D GARNE 2010).

281

282 **3.4. Calibration of the groundwater flow model**

283 The groundwater flow model was calibrated under steady-state conditions corresponding to average
 284 observations for the period 1995-2000. Observations points used for calibration consist in 21
 285 piezometric heads (figure 10) from the monitoring network in Wallonia (DGARNE 2010; Rentier *et al.*
 286 2010) and three baseflow rates estimated using the VCN3 method from hydrographs measured on
 287 streams of the basin. The frequency of hydraulic head measurements was either daily, weekly or
 288 monthly and/or irregularly. Generally, the series contain at least weekly measures for the period 1995-
 289 2000. Each observation was weighted to take into account the quality of the measurement (Hill and
 290 Tiedeman 2007), lower weights being assigned to the base flows since these ones have been
 291 calculated and not measured. The number of calibration points is rather limited given the size of the
 292 basin but there were no other data available than these given by the 21 piezometers. Calibration was
 293 performed by modifying the values of hydraulic conductivity, vertical conductance coefficients of the
 294 clay layer, and exchange coefficients between the Dyle and the Gette basin as well as between rivers
 295 and groundwater.

296

297 The first step of the calibration process consisted in performing a sensitivity analysis using the PEST
 298 code (Doherty 2005). The PEST code calculates the *composite scaled sensitivity (css)*, which is a
 299 measure of the sensitivity of one parameter to all observations (Hill *et al.* 1998; Hill and Tiedeman
 300 2007):

$$css_j = \left[\frac{\sum_{i=1}^{ND} (dss_{ij})^2 |b}{ND} \right]^{1/2}$$

301 where i is the considered observation, j is the considered parameter, ND is the number of
 302 observations, b is the vector containing the values of the parameters for which sensitivities are
 303 analysed and dss is the *dimensionless scaled sensitivity* indicating the importance of an observation
 304 on the estimation of a parameter (USGS, 2006).

305

306 Next to the sensitivity metrics suggest by Hill and Tiedeman (2007), the sensitivity indices presented
 307 by Doherty and Hunt (2009) are worthwhile considering. The parameter *identifiability* value, which
 308 varies between zero and one, with zero indicating complete non-identifiability and one indicating
 309 complete identifiability, is defined as the capability of model calibration to constrain parameters used
 310 by a model (*ibid.*). As seen in Figure 8, the identifiable parameters are quite identical to those defined
 311 as the most sensitive using composite scaled sensitivities.

312 **Figure 7. Composite scale sensitivity values of the parameters**

313 **Figure 8. Parameter identifiability values**

314

315 Thanks to this estimate of the global sensitivity of each parameter, it is possible to select the
316 parameters to be included in the calibration process. A parameter with a css value lower than 1 or
317 lower than 1/100 of the maximum css value is considered as poorly sensitive (Hill and Tiedeman
318 2007). The low sensitive parameters are, in practice, given a fixed value estimated from the
319 hydrogeological database. Consequently, one hydraulic conductivity and two exchange coefficients
320 are fixed according to the values of the literature (Table 2). The composite scale sensitivity values are
321 represented in Figure 7. As the recharge is calculated by WetSpass and prescribed to the
322 groundwater flow and transport models, this parameter is not included in the optimisation process.
323 However, the sensitivity of the recharge is calculated together with the sensitivity of the other
324 parameters for a comparison purpose. As shown in Figure 7, hydraulic heads and discharge rates are
325 very sensitive to the recharge which highlights the necessity of an accurate estimate of this parameter
326 for groundwater flow and transport models.

327

328 The remaining parameters were calibrated using the PEST code, which minimises an objective
329 function representative of the discrepancies between observed values and their simulated equivalent:

$$S(b) = \sum_{i=1}^{ND} \omega_i [y_i - y'_i(b)]^2$$

330 with ND the number of observations, ω_i the i^{th} observation weight, b the parameter, y_i the observed
331 value of the i^{th} observation and y'_i the simulated value associated to the i^{th} observation (Doherty 2005).

332

333 The resulting calibrated parameters for the steady-state calibration are listed in Table 2.

334 **Table 2. Optimized hydraulic conductivity values of the Upper Dyle basin**

335

336 Optimized hydraulic conductivities are in the same order of magnitude as those found in the literature
337 (Dassargues and Monjoie 1993; Dassargues and Ruthy 2001; Peeters 2010). The hydraulic
338 conductivity of Paleozoic and Precambrian bedrock is low but in the range given by Dassargues and
339 Ruthy (2001). The chalk hydraulic conductivity is in the same range than the one given in Dassargues

340 and Monjoie (1993). The three classes of Brussels sands have a similar hydraulic conductivity and
341 their values are closed to the one found in Possemiers *et al.* (2012).

342

343 The calibrated computed heads were compared to the measured heads (Figure 9). The RMS error is
344 8.6 m. This RMS error is still quite high and is certainly due to the assumptions made in the conceptual
345 model (see discussion below). The RMS error obtained for the baseflow is 0.37 m³/s. To further
346 compare the results, it is also interesting to refer to the piezometric map obtained by the 'Bayesian
347 Data Fusion' technique (Peeters 2010) with a large number of observation points (176). The
348 comparison shows that the model gives a good representation of the general configuration of
349 piezometry and the influence of drainage (Figure 10). However, while groundwater flow in the Dyle
350 catchment is highly influenced by the topography, the drainage network is not as pronounced in figure
351 10a and 10b. This is probably due to the use of a finite element mesh composed of relatively large
352 elements and without any refinement along the drainage network.

353

354 **Figure 9. Comparison between observed and computed heads of the groundwater flow model**
355 **of the upper Dyle basin**

356

357 **Figure 10. Comparison of the piezometric maps, a) from Peeters (2010); b) obtained with the**
358 **distributed recharge calculated by WetSpass, and location of observation points used in the**
359 **calibration (in black)**

360

361 **3.5. Implementation of the groundwater nitrate transport model**

362 The nitrate transport model was developed in transient conditions using the calibrated steady-state
363 flow model. The simulation was performed from 1950 to 2010 following three different simple
364 scenarios, represented in Figure 11. Constant nitrate concentrations of 0 mg/L and 10 mg/L are
365 associated to the recharge in urbanised areas and forests respectively. A linear increase of nitrate
366 input between 10 mg/L in 1950 and 50, 60 and 70 mg/L in 1985 is associated to infiltration from
367 cultivated areas (oral communication, Nitrawal organism in Wallonia). After 1985, a constant nitrate
368 input is considered. The simplified nitrate input functions are distributed spatially on the basin,
369 according to land use, as showed in Figure 11. The application of the transport model following the

370 three scenarios shows that scenarios 2 and 3 result in a higher concentration in the south part of the
371 basin (between 47 mg/L and 56 mg/L for scenario 2 and 52 mg/L and 66 mg/L for scenario 3 in 2010)
372 while scenario 1 results in a low concentration for the three dates.

373 **Figure 11. Spatial distribution of the nitrate concentration associated to recharge and**
374 **scenarios for infiltration in cultivated areas**

375 **Figure 12. Concentration in nitrate resulting for the transport model and comparison of the**
376 **results with observation points**

377

378 The results presented in Figure 12 show that the simulated nitrate concentrations are closed to the
379 observed one, either in agricultural areas or in urbanised areas. In comparison with the map published
380 by Mattern (2009), the results of the transport model are in the same order of magnitude and the
381 approach considered here seems satisfactory. The higher nitrate concentrations in the south-eastern
382 part of the basin are well simulated, as well as the lower concentrations in the central zone. However,
383 the results show an overestimation of the nitrate concentration in the south-western part of the basin.

384

385 **4. Discussion**

386 The main objective of this paper was to demonstrate the actual feasibility of linking the WetSpass
387 model with the SUFT3D code in order to simulate the nitrate trend at the regional scale and to
388 illustrate it on the Upper Dyle basin. However, the proposed methodology still contains a series of
389 limitations that are discussed here.

390

391 The WetSpass model presents the advantage of involving most of the parameters influencing the
392 recharge. It is user-friendly and the needed data can be derived from satellite images. Nevertheless,
393 for several data, such as land use, we have chosen to not distinguish the seasons of the year although
394 the WetSpass model can differentiate two seasons (summer and winter). It may present limitations
395 since seasonal variations influence land use, especially during cultural practices. However, these
396 possible effects are limited since WetSpass allows taking into account several parameters varying
397 from summer to winter (vegetated area, interception percentage, bare area ...). Finally, as previously
398 mentioned, maize and tuberous cultures can have a great influence on recharge and its spatial
399 distribution. Considering the crops of one year cannot be representative enough for providing reliable

400 long term mean recharge. However, it has been shown that this has not a great effect on the mean
401 annual recharge since almost 80% of the differences between recharge resulting from either 2008 or
402 2009 crops are in a range of 15 mm/year.

403

404 Concerning the groundwater flow model, the RMS error obtained after the calibration process remains
405 quite high. Several conceptual choices may be discussed considering, for example, a finer zonation of
406 the Brussels sands, more detailed data about the distribution and the thickness and the hydraulic
407 conductivity of the clay layer. Moreover, observed values are considered as to be compared to steady
408 state simulated values. Additionally, the observed values are also compared with computed values at
409 the nearest node and consequently, different values of groundwater level observed in different but
410 very close wells can be actually compared to a unique computed value (Orban, 2008). Finally, the
411 number of piezometers used for the calibration remains here very limited. Indeed, a higher number of
412 piezometric data could potentially improve the model calibration.

413

414 The spatial distribution of nitrate inputs generated interesting results. However, the transport model
415 was here not calibrated because of the lack of distributed and temporal data. The land use spatial
416 distribution was also considered as constant over time but it is likely that it varied between 1950 and
417 2010 and it will vary in the future. Another simplification concerns the stationary hydrological regime as
418 this study focuses on long-term general nitrate trends in the aquifer that can be (in a first stage)
419 considered as weakly influenced by short-term cyclic variation of groundwater levels.

420

421 **5. Conclusion**

422 The work presented here demonstrates the feasibility of developing an integrated water and nitrate
423 transport model at the regional scale. The practical application of the method is shown on the case
424 study of the Upper Dyle basin. This integrated model is based on the association of the WetSpass
425 model (water balance model) and the SUFT3D code (groundwater flow and transport model), where
426 the outputs of the former model in terms of recharge are used as inputs by the latter model. The
427 groundwater flow and nitrate transport model developed with the SUFT3D and its innovative HFEMC
428 technique is based on detailed regional hydrogeological conditions and time and space distribution of

429 nitrate in groundwater. Even if a series of simplification have been considered and discussed, results
430 seem to be reliable and using WetSpass clearly improved the results of the groundwater flow model.

431

432 There are several perspectives to the methodology proposed in this paper. The WetSpass model and
433 the SUFT3D code can be used in this way for a non stationary groundwater flow instead of a steady-
434 state model. Land use and climatic changes in the future could also be considered in the scenarios to
435 be modelled and should result in more realistic previsions. In terms of groundwater resources
436 management, such a work could provide further very useful information for decisions makers. Other
437 scenarios can be included (in terms of nitrate concentrations evolution, for example) and used to
438 forecast groundwater behaviour in response to the political decisions considered or undertaken. Such
439 a tool is thus of major interest to support groundwater managers in charge of the implementation of
440 regulations (for example the European Water Framework Directive) on groundwater quality with
441 respect to diffuse contamination issues such as nitrate from agriculture.

442

443 **6. References**

444 Amin I E, Campana M E (1996) A general lumped parameter model for the interpretation of tracer data
445 and transit time calculation in hydrologic systems. *J Hydro* 179: 1-21

446

447 Barrett M E, Charbeneau R J (1996) A parsimonious model for simulation of flow and transport in a
448 karst aquifer, Center for Research in Water Resources, Bureau of Engineering Research, The
449 University of Texas at Austin, Austin

450

451 Barthel R, Jagelke J, Götzinger J, Gaiser T, Printz A (2008) Aspects of choosing appropriate concepts
452 for modelling groundwater resources in regional integrated water resources management - Examples
453 from the Neckar (Germany) and Ouémé catchment (Benin). *Phys Chem Earth* 33(1-2): 92-114

454

455 Batelaan O, De Smedt F (2001) WetSpass: a flexible, GIS based, distributed recharge methodology
456 for regional groundwater modelling. In: Gehrels H, Peters J, Hoeh, E, Jensen K, Leibundgut C,
457 Griffioen J, Webb B, Zaadnoordijk WJ (eds), *Impact of Human Activity on Groundwater Dynamics*,
458 269, IAHS, Wallingford, 11-17

459

460 Batelaan O, De Smedt F (2004) Seepage, a new modflow drain package. *Ground Water* 42(4): 576–
461 588.

462

463 Batelaan O, De Smedt F (2007) GIS-based recharge estimation by coupling surface-subsurface water
464 balances. *J Hydro* 337: 337-355

465

466 Batelaan O, Woldeamlak S T (2007) *ArcView Interface for WetSpass, User Manual, Version 13-06-*
467 *2007, Vrije Universiteit Brussel (BE), Department of Hydrology and Hydraulic Engineering, 75 p.*

468

469 Brouyère S (2001) *Etude et modélisation du transport et du piégeage des solutés en milieu souterrain*
470 *variablement saturé (Study and modeling of solutes transport and trapping in variably saturated*
471 *underground environment). PhD. University of Liège, 640p.*

472

473 Brouyère S, Carabin G, Dassargues A (2004) Climate change impacts on groundwater resources:
474 modelled deficits in a chalky aquifer, Geer basin, Belgium. *Hydrogeol J* 12: 123-134

475

476 Brouyère S, Orban P, Wildemeersh S, Couturier J, Gardin N, Dassargues A (2009) The Hybrid Finite
477 Element Mixing Cells Method: A new flexible method for modelling mine ground water problems. *Mine*
478 *Water Environ* 28(2): 102-114

479

480 Brunner P, Simmons C T (2012) HydroGeoSphere: A Fully Integrated, Physically Based Hydrological
481 Model. *Ground Water* 5(2): 170-176

482

483 Campana M E, Sadler N, Ingraham N L, Jacobson R L (1997) A deuterium-calibrated compartmental
484 model of transient flow in a regional aquifer system. *Tracer Hydro*: 389-396

485

486 Carabin G, Dassargues A (1999) Modeling groundwater with ocean and river interaction. *Water*
487 *Resour Res* 35(8): 2347-2358

488

489 Celia M A, Bouloutas E T, Zarba R L (1990) A general mass-conservative numerical solution for the
490 unsaturated flow equation. *Water Resour Res* 26(7): 1483-1496
491

492 Christakos G, Bogaert P (1996) Spatiotemporal analysis of spring water ion processes derived from
493 measurements at the Dyle Basin in Belgium. *IEEE Transactions On Geoscience And Remote Sensing*
494 34(3): 626–642
495

496 Collins A L, McGonigle D F (2008) Monitoring and modelling diffuse pollution from agriculture for policy
497 support: UK and European experience. *Environ Sci & Policy* 11(2): 97-101
498

499 Dams J, Woldeamlak S T, Batelaan O (2007) Forecasting land-use change and its impact on the
500 groundwater system of the Kleine Nete catchment, Belgium, *Hydro & Earth Syst Sci Discuss* 4: 4265–
501 4295
502

503 Dassargues A, Brouyère S, Monjoie A, (2001) Integrated modelling of the hydrological cycle in relation
504 to global climate change, Groundwater sub-models, Final report, SSTC-BELSPO (Belgium Federal
505 Scientific Policy), Program Global Change - Sustainable Development. 19 p.
506

507 Dassargues A, Monjoie A (1993) Les aquifères crayeux en Belgique (The chalky aquifers of Belgium).
508 *Hydrogéologie* 2: 135-145
509

510 Dassargues A, Radu J P, Charlier R (1988) Finite elements modelling of a large water table aquifer in
511 transient conditions. *Adv Water Res* 11(2): 58-66
512

513 Dassargues A, Ruthy I (2001) Carte hydrogéologique de Wallonie (Hydrogeological map of Walloon
514 Region), Chastre - Gembloux, 49/5-6 1/25000, Ministry of Walloon Region, DGARNE.
515

516 Dassargues A, Ruthy I (2002) Carte hydrogéologique de Wallonie (Hydrogeological map of Walloon
517 Region), Chastre - Gembloux, 40/1-2 1/25000, Ministry of Walloon Region, DGARNE.
518

519 De Vries J J, Simmer I (2002) Groundwater recharge: an overview of processes and challenges.
520 *Hydrogeol J* 10: 5-17
521
522 DGARNE (2010) Etat des nappes d'eau souterraines de la Wallonie (State of groundwater in
523 Wallonia). In Walloon Region (Belgium), <http://environnement.wallonie.be/de/eso/atlas>. Cited in
524 February 2013
525
526 Diekkrüger B, Sondgerath D, Kersebaum K C, McVoy C W (1995) Validity of agro-ecosystem models-
527 a comparison of different models applied to the same data set. *Ecol Modell* 81(13): 3-29.
528
529 Doherty J (2005) PEST – Model-Independent parameter estimation – User manual – 5th edition.
530 Watermark Numerical Computing
531
532 Doherty J, Hunt R J (2009) Two statistics for evaluating parameter identifiability and error reduction. *J*
533 *Hydro* 366: 119-127
534
535 Duffy C J, Lee D H (1992) Base flow response from non-point source contamination: spatial variability
536 in source, structure, and initial condition. *Water Resour Res* 28(3): 905-914
537
538 Goderniaux P, Brouyère S, Fowler H J, Blenkinsop S, Therrien R, Orban Ph, Dassargues A (2009)
539 Large scale surface – subsurface hydrological model to assess climate change impacts on
540 groundwater reserves. *J Hydro* 373: 122-138
541
542 Goderniaux P, Brouyere S, Blenkinsop S, Burton A, Fowler H J, Orban Ph and Dassargues A (2011)
543 Modelling climate change impacts on groundwater resources using transient stochastic climatic
544 scenarios. *Water Resour Res* 47(12): 1-17
545
546 Habils F, Rorive A (2005) Carte hydrogéologique de Wallonie (Hydrogeological map of Walloon
547 Region), Nivelles – Genappes, 39/7-8 1/25000, Ministry of Walloon Region, DGARNE.
548

549 Hallberg K B, Keeney D R (1993) Nitrate. In: Alley W M (ed) Regional Ground-Water quality, Van
550 Nostrand Reinhold, New York
551
552 Harrington G A, Walker G R, Love A J, Narayan K A (1999) A compartmental mixing-cell approach for
553 the quantitative assessment of groundwater dynamics in the Otway Basin, South Australia. *J Hydro*
554 214: 49-63
555
556 Harter T, Davis H, Mathews M C, Meyer, R D (2002) Shallow ground water quality on dairy farms with
557 irrigated forage crops. *J Contam Hydro* 55: 287-315
558
559 Healy R W (2010) *Estimating groundwater recharge*. Cambridge University Press, Cambridge
560
561 Henriksen H J, Trolborg L, Nyegaard P, Sonnenborg T O, Refsgaard J C, Madsen B (2003)
562 Methodology for construction, calibration and validation of a national hydrologic model for Denmark. *J*
563 *Hydro* 280: 52-71
564
565 Hill M C, Tiedeman C R (2007) *Effective Groundwater Model Calibration: With Analysis of Data,*
566 *Sensitivities, Predictions, and Uncertainty*. John Wiley & Sons, Inc, Hoboken
567
568 Hill M, Colley R, Pollock D (1998) A controlled experiment in groundwater flow model calibration using
569 nonlinear regression. *Ground Water* 36(3): 520-535
570
571 Houthuys R (2011) A sedimentary model of the Brussels Sands, Eocene, Belgium. *Geologica Belgica*
572 14
573
574 Hudak P F (2000) Regional trends in nitrate content of Texas groundwater. *J Hydro* 228: 37-47
575
576 Jackson B M, Browne C A, Butler A P, Peach D, Wade A J, Wheeler H S (2008) Nitrate transport in
577 Chalk catchments: monitoring, modelling and policy implications. *Environ Sci & Policy* 11(2): 125-135
578

579 Jenifa Lata C, Saravanan S, Palanichamy K (2010) A semi-distributed water balance model for
580 Amaravathi river basin using remote sensing and GIS. *Int J Geomat & Geosci* 1(2): 252-263
581

582 Johnsson H, Larsson M, Martensson K, Hoffmann M (2002) SOILNDB: a decision support tool for
583 assessing nitrogen leaching losses from arable land. *Environ Model & Softw* 17(6): 505-517
584

585 Jury W A (1982) Simulation of solute transport using a transfer function model. *Water Resour Res*
586 18(2): 363-368
587

588 Laurent E (1978) Monographie du bassin de la Dyle (Dyle Basin monograph), Ministry of Public Health
589 and Environment, 302 p.
590

591 Ledoux E, Gomez E, Monget J M, Viavattene C, Viennot P, Ducharne A, Benoit M, Mignolet C, Schott
592 C Mary B (2007) Agriculture and groundwater nitrate contamination in the Seine basin. The STICS-
593 MODCOU modelling chain. *Sci Total Environ* 375: 33-47
594

595 Maloszewski P, Zuber A (1982) Determining the turnover time of groundwater systems with the aid of
596 environmental tracers. 1. Models and their applicability. *J Hydro* 57: 207-231
597

598 Mattern S (2009) *Mapping and source identification of groundwater pollution by nitrate. Theory and*
599 *application to the Brusselian sand groundwater body*. PhD. Catholic University of Louvain, 236p.
600

601 Mattern S, Fasbender D, Vanclooster M (2009) Discriminating sources of nitrate pollution in an
602 unconfined sandy aquifer. *J Hydro* 376: 275-284
603

604 Mitchell R J, Scott Babcock R, Gelinas S, Nanus L, Stasney D E (2003) Nitrate distributions and
605 source identification in the Abbotsford-Sumas aquifer, Northwester Washington state. *J Environ Qual*
606 32: 789-800
607

608 Mohamed M A A, Terao H, Suzuki R, Babiker I S, Ohta K, Kaori K, Kato K (2003) Natural
609 denitrification in the Kakamigahara ground water basin, Gifu prefecture, central Japan. *Sci Total*
610 *Environ* 307: 191-201
611
612 Navarre A, Lecomte P, Martin H (1976) Analyse des tendances de données hydrochimiques du bassin
613 de la Dyle en amont d'Archennes. *Annales de la Société Géologique de Belgique* 99: 299-313
614
615 Orban Ph (2008) *Solute transport modeling at the groundwater body scale : nitrates trends*
616 *assessment in the Geer basin (Belgium)*. PhD. University of Liège, 207p.
617
618 Orban Ph, Brouyère S, Battle-Aguilar J, Couturier J, Goderniaux P, Leroy M, Malozewski P,
619 Dassargues A (2010) Regional transport modelling for nitrate trend assessment and forecasting in a
620 chalk aquifer. *J Contam Hydro* 118: 79-93
621
622 Orban Ph, Brouyère S, Wildemeersch S, Couturier J, Dassargues A (2008) The hybrid Finite-Element
623 Mixing-Cell method : a new flexible method for large scale groundwater modelling, *CMWR XVII -*
624 *Computational Methods in Water Resources*. San Francisco: USA, July 2008.
625
626 Oren O, Yechieli Y, Böhlke J K, Dody A (2004) Contamination of groundwater under cultivated fields in
627 a arid environment, central Arava Valley, Israel. *J Hydro* 290: 312-328.
628
629 Peeters L (2010) *Groundwater and geochemical modelling of the unconfined Brussels aquifer,*
630 *Belgium*. PhD. Catholic University of Leuven, 232p.
631
632 Pineros Garcet J, Ordonez A, Roosen J, Vanclooster M (2006) Metamodelling: theory, concepts and
633 application to nitrate leaching modelling, *Ecological Modelling* 193: 629-644
634
635 Possemiers M, Huysmans M, Peeters L, Batelaan O, Dassargues A. (2012) Relationship between
636 sedimentary features and permeability at different scales in the Brussels Sands. *Geologica Belgica*
637 15(3): 156-164

638

639 Meyus Y, Woldeamlak S T, Batelaan O, De Smedt F (2004) Opbouw van een Vlaams
640 Grondwatervoedingsmodel: Eindrapport (Structure of a Flemish Groundwater Model: Final Report),
641 Technical Report 81p., AMINAL, afdeling Water.

642

643 Peeters L, Bação F, Lobo V, Dassargues A (2007) Exploratory data analysis and clustering of
644 multivariate spatial hydrogeological data by means of GEO3DSOM, a variant of Kohonen's Self-
645 Organizing Map. *Hydro & Earth Syst Sci* 11: 1309-1321

646

647 Peeters L, Fasbender D, Batelaan O, Dassargues A (2010) Bayesian Data Fusion for water table
648 interpolation: incorporating a hydrogeological conceptual model in kriging. *Water Resour Res* 46 (8):
649 W08532.

650

651 Rentier C, Delloye F, Brouyère S, Dassargues A (2006) A framework for an optimised groundwater
652 monitoring network and aggregated indicators. *Environ Geol* 50(2): 194-201

653

654 Rozos E, Koutsoyiannis D (2006) A multicell karstic aquifer model with alternative flow equations. *J*
655 *Hydro* 325: 340-355

656

657 Scanlon B R, Healy R W, Cook P G (2002) Choosing appropriate techniques for quantifying
658 groundwater recharge. *Hydrogeol J* 10: 18-39

659

660 Skaggs T H, Kabala Z J, Jury W A (1998) Deconvolution of a nonparametric transfer function for
661 solute transport in soils. *J Hydro* 207: 170-178

662

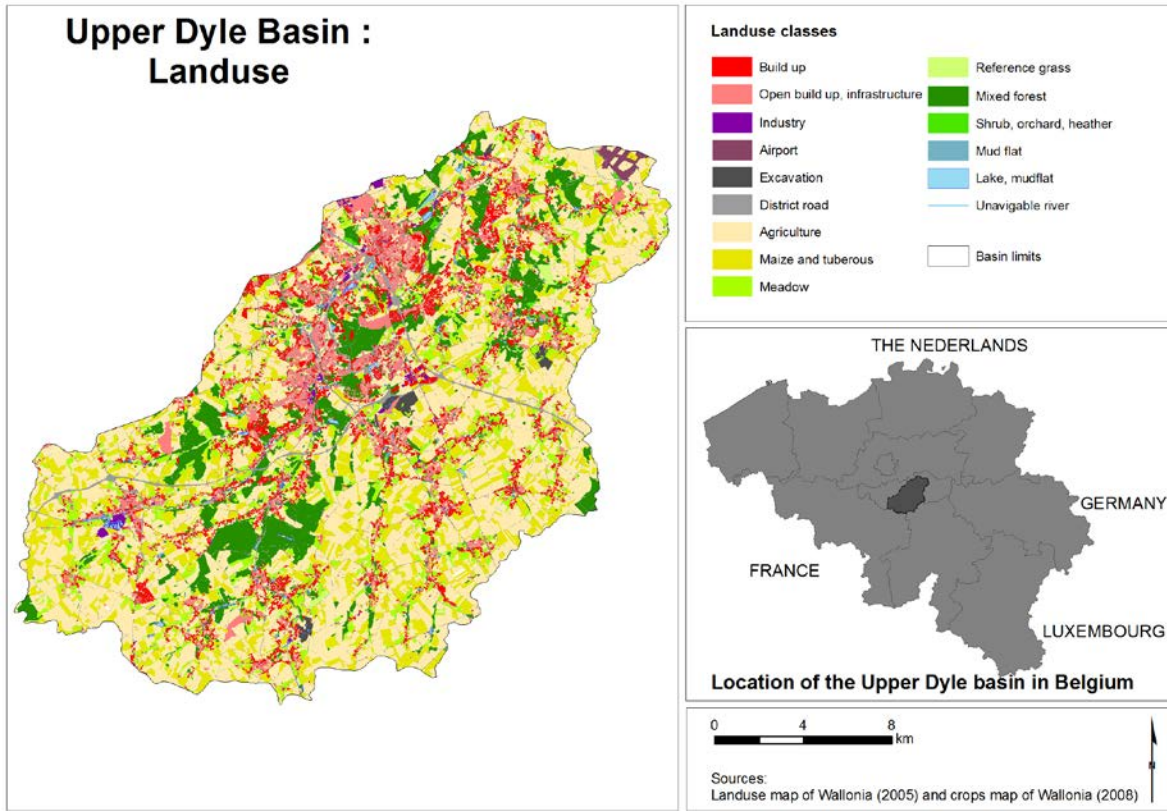
663 Sohier C, Degré A, Dautrebande S (2009) From root zone modelling to regional forecasting of nitrate
664 concentration in recharge flows – The case of the Walloon Region (Belgium). *J Hydro* 369: 350-359

665

666 Sophocleous M, Koelliker J K, Govindaraju R S, Birdie T, Ramireddygar S R Perkins S P (1999)
667 Integrated numerical modeling for basin-wide water management: The case of the Rattlesnake Creek
668 basin in south-central Kansas. *J Hydro* 214: 179-196
669
670 Stewart I T, Loague K (1999) A type transfer function approach for regional-scale pesticide leaching
671 assessments. *J Environ Qual* 28(2): 378-387
672
673 Sutton M, Howard C, Erisman J W, Billen G, Bleeker A, Grennfelt P, van Grinsven H, Grizzetti B (ed)
674 (2011). The European Nitrogen Assessment: sources, effects and policy perspectives. Cambridge
675 University Press. Cambridge
676
677 Therrien R, Sudicky E A (1996) Three-dimensional analysis of variably-saturated flow and solute
678 transport in discretely-fractured porous media. *J Contam Hydro* 23(1-2): 1-44
679
680 Therrien R, Sudicky E, McLaren R, Panday S (2005) HydroGeoSphere – A three-dimensional
681 numerical model describing fully-integrated subsurface and surface flow and solute transport. Manual,
682 Groundwater Simulations Group
683
684 Thorburn P J, Biggs J S, Weier K L, Keating B A (2003) Nitrate in ground waters of intensive
685 agricultural areas in coastal Northeastern Australia. *Agriculture, Ecosyst & Environ* 94: 49-58
686
687 USGS (2009) Methods for estimating groundwater recharge in humid regions.
688 <http://water.usgs.gov/ogw/gwrp/methods/>. Cited in February 2013
689
690 Visser A, Dubus I, Broers H P, Brouyere S, Korcz M, Orban Ph, Goderniaux P, Batlle-Aguilar J,
691 Surdyk N, Amraoui N, Job H, Pinault J L, Bierkens M (2009) Comparison of methods for the detection
692 and extrapolation of trends in groundwater quality. *J Environ Monit* 11: 2030-2043
693
694 Walloon Region (2005) Etat des lieux des sous-bassins hydrographiques, Tome 1 : Etat des lieux.
695 Sous-bassin Dyle-Gette. Description générale des caractéristiques du sous-bassin (Inventory of

696 subwatershed, Volume 1: Inventory. Dyle-Gette subwatershed. General description of the
697 subwatershed characteristics), In Walloon Region.
698 http://environnement.wallonie.be/directive_eau/edl_ssb/dg/Dg1.pdf. Cited in February 2013.
699
700 Wang Y, Lei X, Liao W, Jiang Y, Huang X, Liu J, Song X, Wang (2012) Monthly spatial distributed
701 water resources assessment: a case study. *Comput & Geosci* 45: 319-330
702
703 Wick K, Heumesser C, Schmid E (2012) Groundwater nitrate contamination: Factors and indicators. *J*
704 *Environ Manag* 111: 178-186
705
706 Wildemeersch S, Brouyère S, Orban Ph, Couturier J, Dingelstadt C, Veschkens M, Dassargues A
707 (2010) Application of the Hybrid Finite Element Mixing Cell method to an abandoned coalfield in
708 Belgium. *J Hydro* 392(3-4): 188-200
709
710 Yi M J, Lee K K (2004) Transfer function-noise modelling of irregularly observed groundwater heads
711 using precipitation data. *J Hydro* 288: 272-287

1

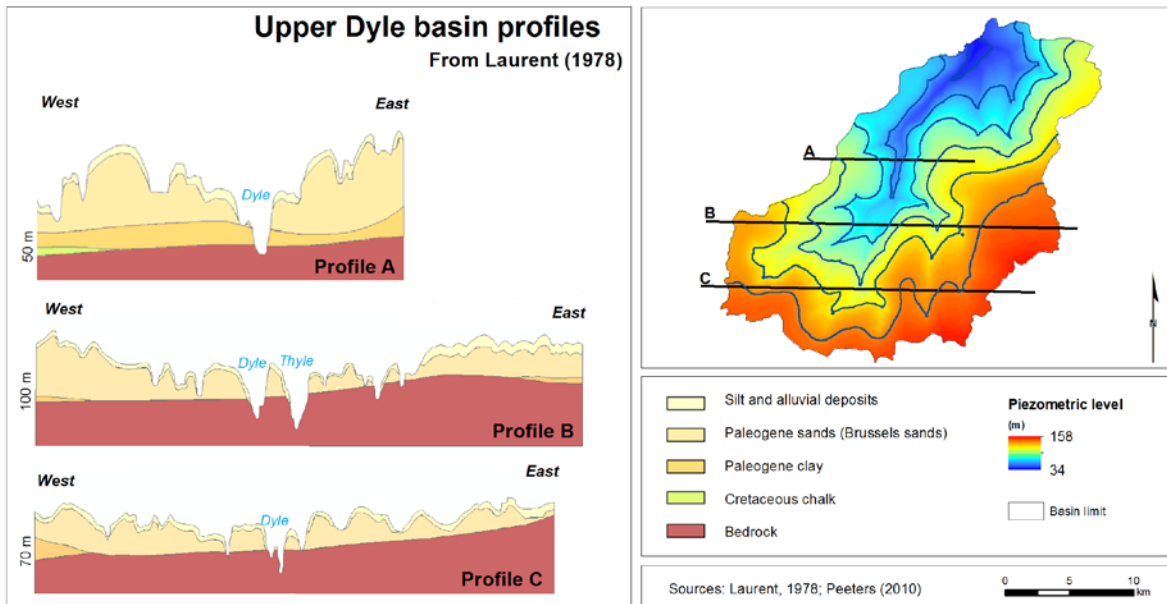


2

3

4

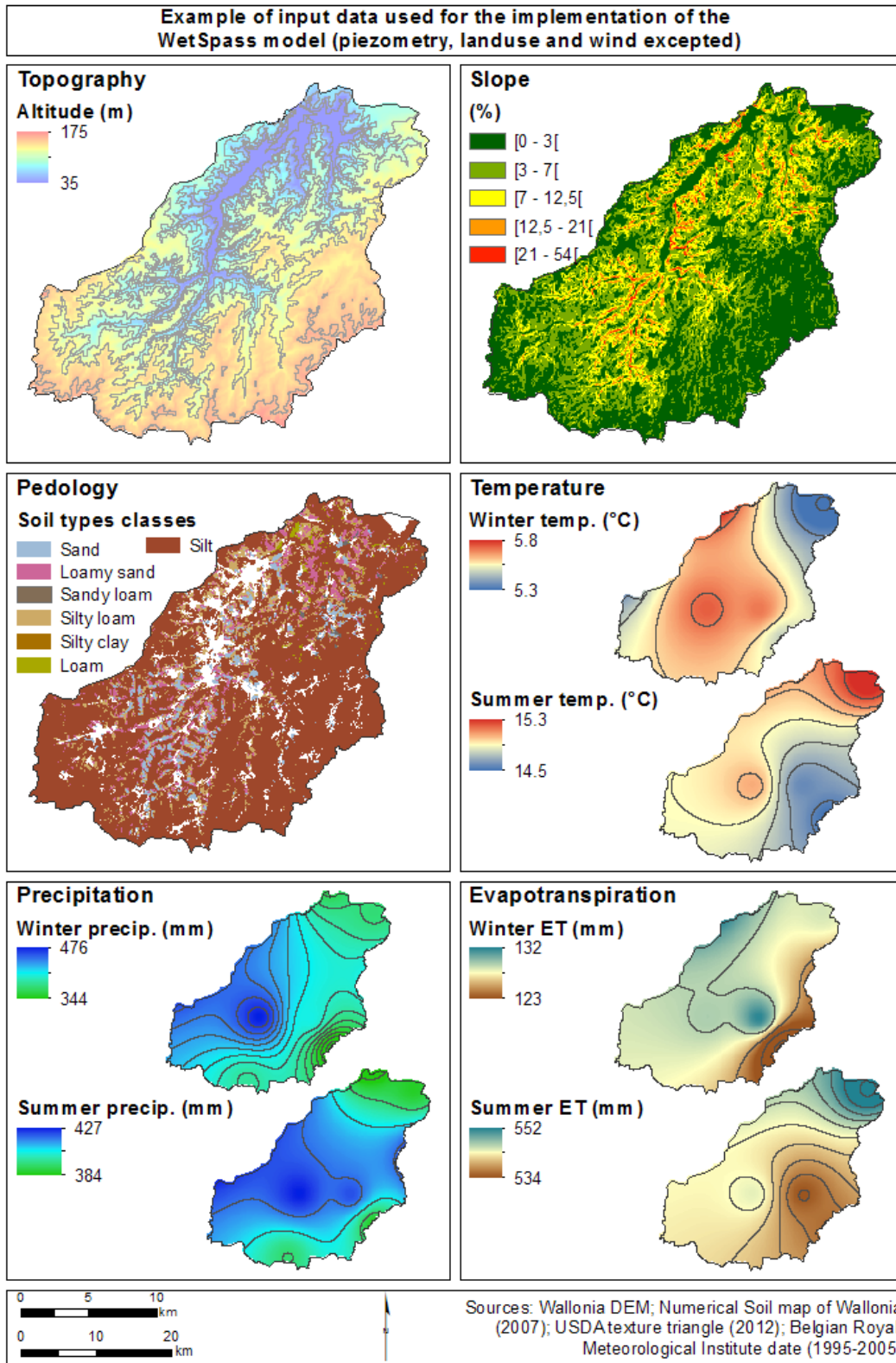
Figure 1. Landuse and location of the upper Dyle basin



5

6

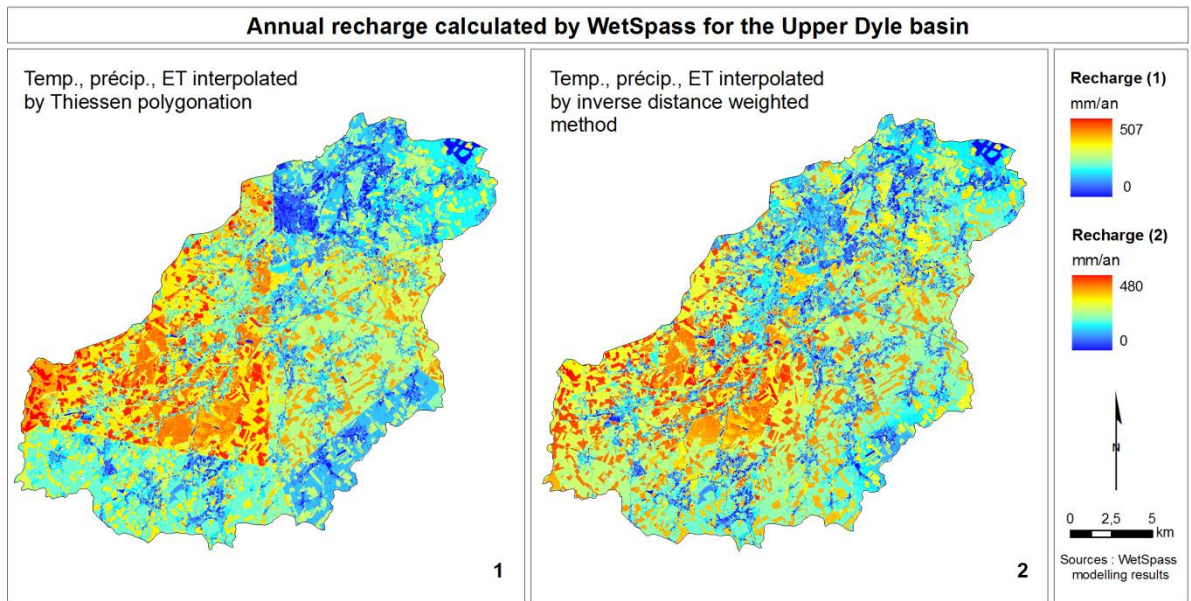
Figure 2. Typical profiles in the upper Dyle basin



7

8

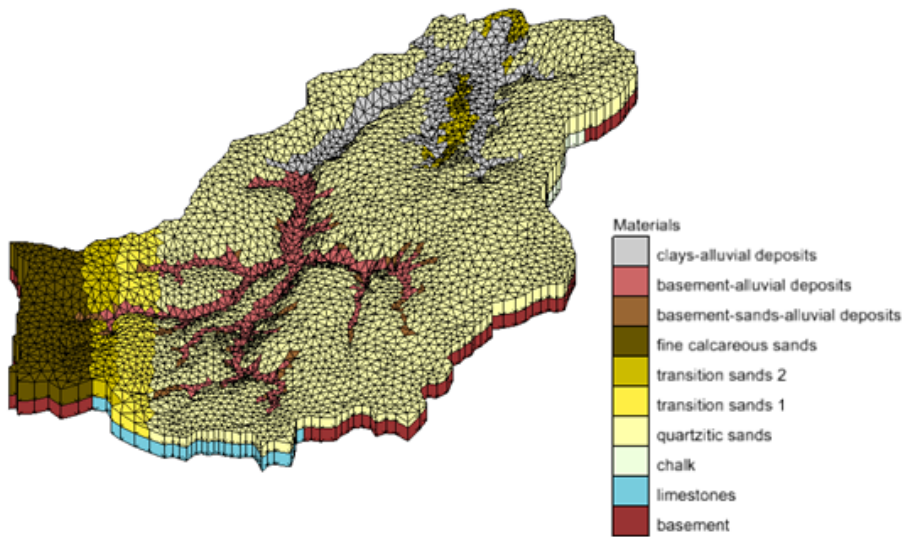
Figure 3. Example of input raster data of the WetSpass model



9

10

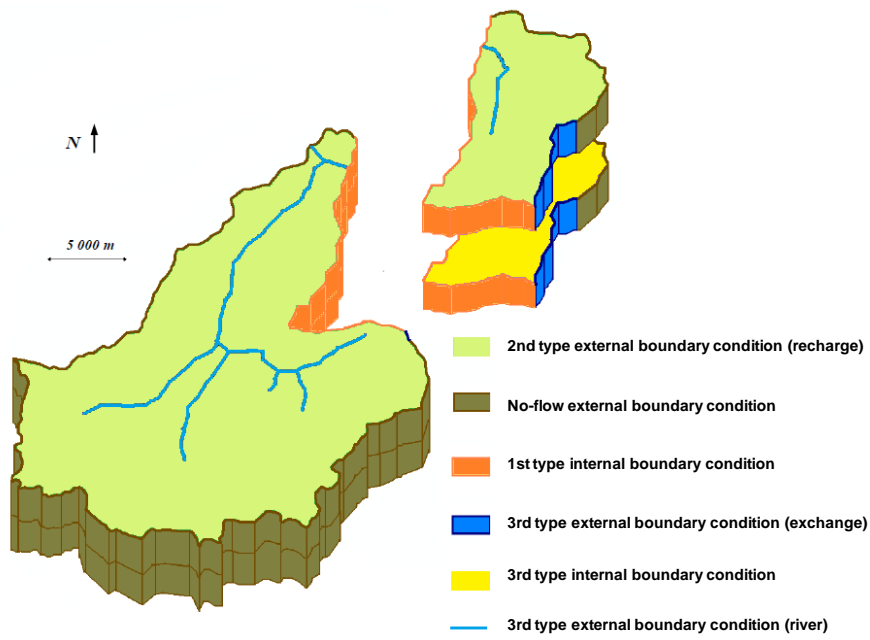
Figure 4. Annual recharge calculated by the WetSpass model for two combinations of inputs



11

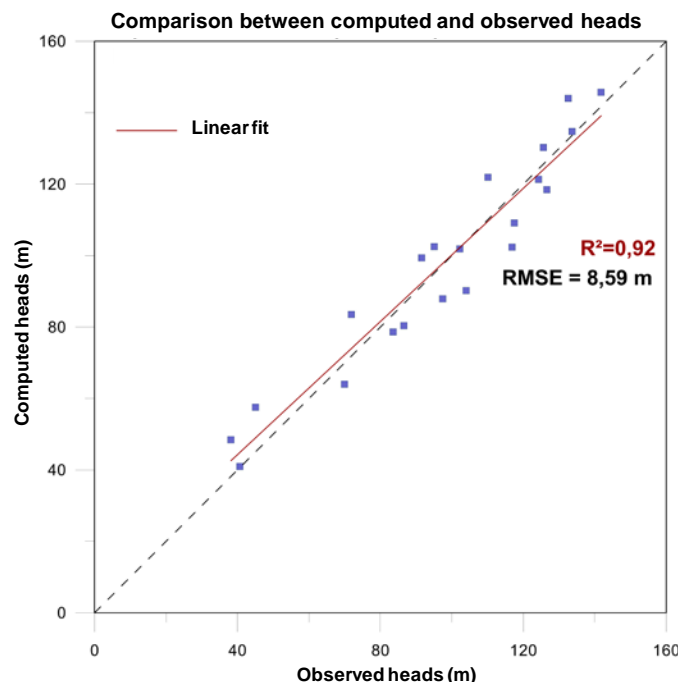
12

Figure 5. 3D finite element mesh and zonation used for the groundwater modelling



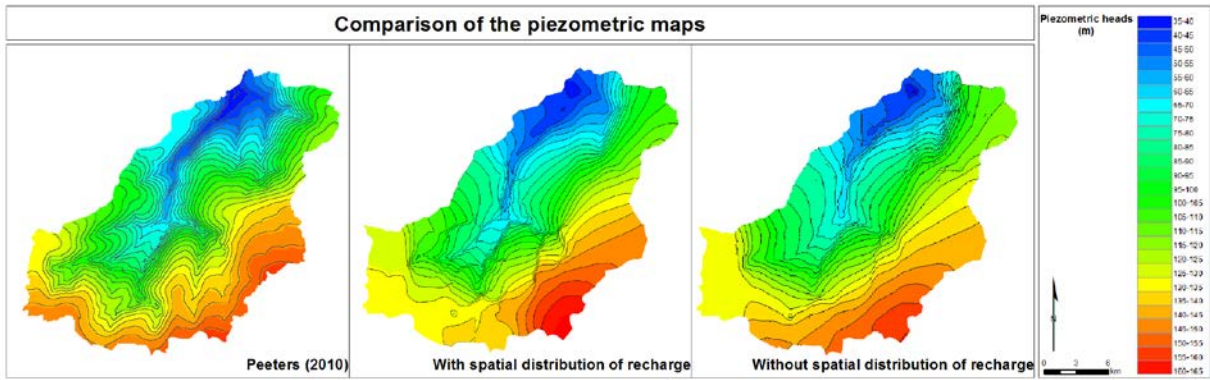
13
14
15

Figure 6. Internal and external boundary conditions



16
17

Figure 7. Comparison between observed and computed heads



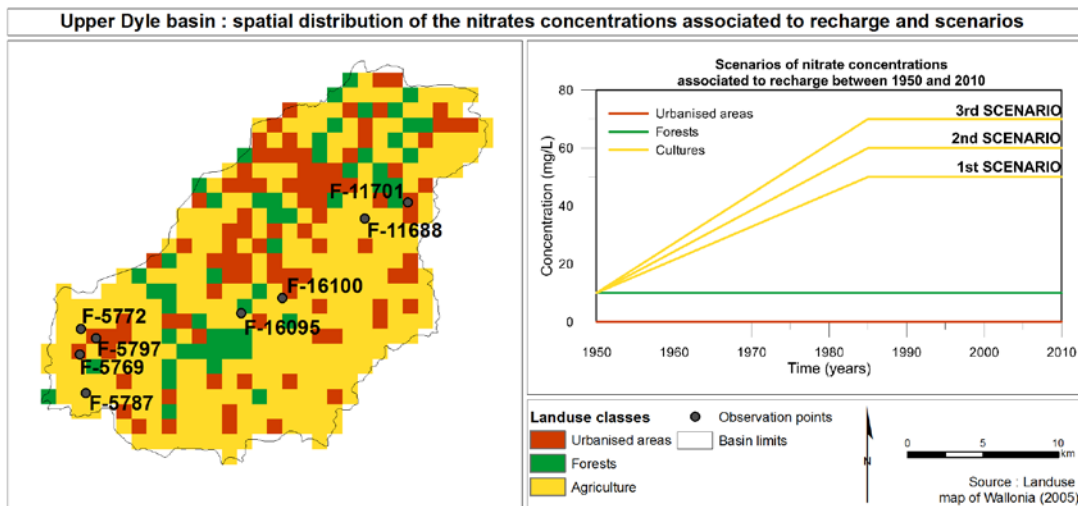
18

19

20

21

Figure 8. Comparison of the piezometric maps, a) of Peeters (2010) ; b) obtained with an uniform recharge ; c) obtained with the distributed recharge calculated by WetSpass

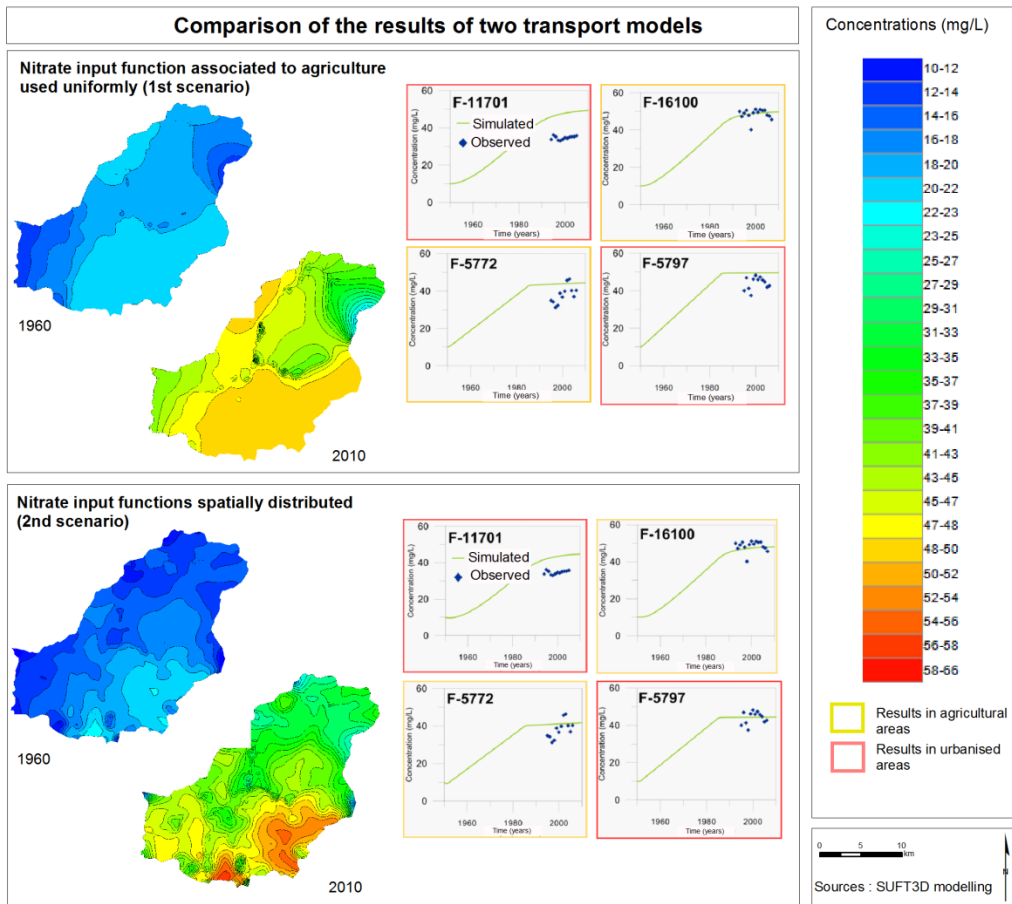


22

23

24

Figure 9. Spatial distribution of the nitrate concentration associated to recharge



25
26
27
28
29
30
31

Figure 10. Comparison between the results of two transport models implemented with either a spatial distribution of nitrate input or a uniform of nitrate inputs

Table 1. Data needed and methods used to estimate inputs

Wetspass input	Data needed	Method used to estimate input
Topography and slopes	DEM provided by the Belgian National Geographic Institute	Resampling using the nearest neighbour technique to obtain a 10 m resolution, slopes calculation
Pedology	Soil map of Wallonia (2007), USDA texture triangle (2012)	Classification to fit the USDA classification
Landuse	Landuse map (2005) and crops map (2008) of Wallonia	Classification into 20 final classes used by WetSpass

Precipitation and temperature	Monthly average data in nine weather stations, provided by the Meteorological Royal Institute for the period from 1995 to 2005	Two interpolations techniques tested : inverse distance weighted interpolation and Thiessen polygonation
Potential evapotranspiration		Thornthwaite method employed to calculate evapotranspiration at the weather stations and the two previous interpolation techniques were then implemented
Wind		Wind set at a constant value for the whole basin
Piezometry	Piezometric map calculated by Peeters (2010)	"Bayesian data fusion" (Peeters, 2010)

32

33

Table 2. Optimized hydraulic conductivity values of the upper Dyle basin

Parameter	Hydraulic conductivity (m/s)
k1 - Basement	4.2×10^{-06} (optimised)
k2 - Chalk	8.1×10^{-05} (optimised)
k3 - Limesotne	5.0×10^{-03} (optimised)
k4 – Quartzitic sands	2.0×10^{-04} (optimised)
k5 - Clay/Alluvions	2.2×10^{-04} (optimised)
k6 - Basement/Alluvions	1.4×10^{-05} (optimised)
k7 – Basement/Sand/Alluvions	5.0×10^{-07} (fixed)
k8 - Sand 2	1.3×10^{-04} (optimised)
k9 – Sand 1	5.8×10^{-04} (optimised)
k10 – Calcareous fine sand	1.0×10^{-02} (fixed)
Exchange coeff. between groundwater and surface water	9.0×10^{-08} (optimised, mean)
Exchange coeff. between Dyle and Gette basin	1.0×10^{-03} (fixed)
Vertical exchange coeff., with clay	1.1×10^{-10} (fixed)
Vertical exchange coeff., without clay	1.0×10^{-03} (fixed)

34

35